ISSN 1990-7931, Russian Journal of Physical Chemistry B, 2018, Vol. 12, No. 5, pp. 869–874. © Pleiades Publishing, Ltd., 2018.
Original Russian Text © D.A. Sidorenko, P.S. Utkin, 2018, published in Khimicheskaya Fizika, 2018, Vol. 37, No. 9, pp. 43–49.

COMBUSTION, EXPLOSION, AND SHOCK WAVES

Two-Dimensional Gas-Dynamic Modeling of the Interaction of a Shock Wave with Beds of Granular Media

D. A. Sidorenko[a] and P. S. Utkin[a, *]

[a] *Institute for Computer Aided Design, Russian Academy of Sciences, Moscow, 123056 Russia*

**e-mail: pavel_utk@mail.ru*

Received December 13, 2017

Abstract—A two-dimensional numerical parametric study is made of the interaction of a shock wave with a system of cylinders modeling a bed of a granular medium. The mathematical model is based on the Euler equations. The integration of the defining system of equations in a multiply connected domain is taken using an original computational algorithm of the Cartesian grid method. Computational experiments are carried out with various values for bed permeability and length, the diameter of the cylinder, and channel width. The formulation of the problem imitates natural experiments. The results of all the computational experiments in terms of overpressure behind the reflected and transmitted waves are generalized using a dimensionless criterion. The calculated results are compared with the data from the natural experiments.

Keywords: mathematical modeling, shock wave, particle bed, granular media, Euler equations, Cartesian grid method

DOI: 10.1134/S1990793118050111

INTRODUCTION

Multidimensional gas-dynamic modeling is used to refine the qualitative and (less frequently) quantitative characteristics of shock-wave processes in two-phase media [1]. A few recent examples can be given. Bedarev et al. [2] considered a lattice of immobile transverse cylinders, with classified types of interactions of detached shock waves, and demonstrated that the wave patterns emerging in the flows past a cylinder and a sphere significantly differ. Bedarev and Fedorov [3] analyzed the case of two immobile spheres (two-dimensional calculations in the axisymmetric formulation) aligned with the propagation direction of a shock wave, obtaining the drag coefficient versus time curves at various distances between the spheres. Regele et al. [4] used two-dimensional gas–dynamic calculations for quantitative description of multidimensional effects in the interaction of a shock wave with a cloud of particles in the three-dimensional case. This solution was used as an exact solution for subsequent comparison with the results of one-dimensional calculations. These results showed the importance of multidimensional effects related to Reynolds stresses within the particle cloud and in the turbulent wake. Despite the progress in computational experiment methods, such studies in three-dimensional statement are still scarce. Mehta et al. [5] calculated the drag coefficients of the spheres as functions of time in the case of a regular array of immobile spheres by solving the three-dimensional Euler equations with a detailed grid resolution and determined the integral characteristics of the transmitted and reflected waves.

An important aspect influencing the possibility such multidimensional gas–dynamic modeling is the computational algorithm: gas–dynamic equations are solved in a multiply connected domain, which cannot be covered by a structured computational grid. Bedarev et al. [2, 3] made their calculations using the ANSYS Fluent software; the computational grids in the two-dimensional case were tetragonal; no details of the grid design in the multiply connected domain or any relevant features of the computational algorithm were not presented. Regele et al. [4] used a square computational grid and the standard Riemann Solver. Thus, the boundaries of the bodies were obtained stepwise, which could generate artificial nonphysical perturbations. The results presented in this work were obtained using a computational algorithm of the Cartesian grid method for numerical integration of gas–dynamic equations in domains of complex shape [6].

The problem of the interaction of a shock wave with a system of bodies has practical importance in the context of the suppression of shock waves during emergencies in mines [7, 8]. The solution to this problem is also useful for better understanding the mechanisms of propagation of combustion waves in porous media [9].

In this work, we made a parametric numerical study of the interaction of a shock wave with a system of cylinders, which qualitatively imitated natural experiments tests [7] of shock wave attenuation in beds of granular

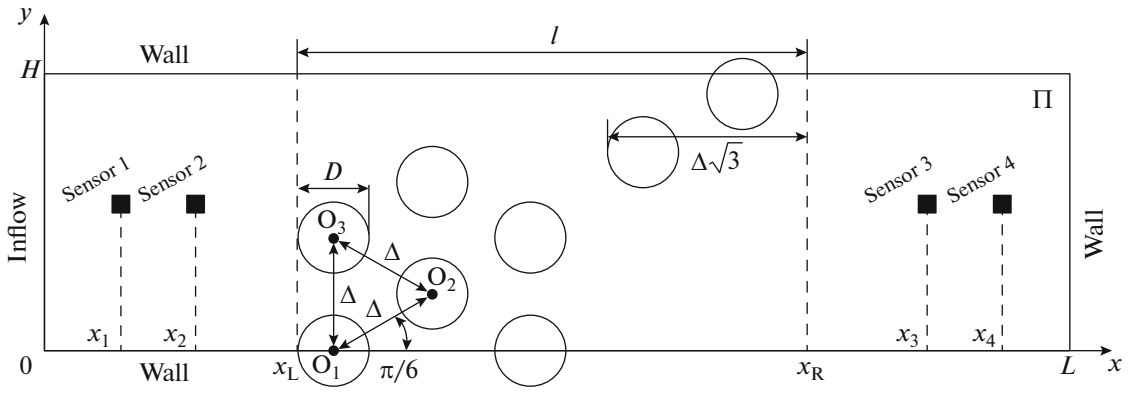

Fig. 1. Schematic of the computational domain.

materials, with varying determining geometric parameters for the problem.

FORMULATION OF THE PROBLEM

The extended computational domain is rectangle Π of length L and width H in Cartesian coordinate system (x, y), which is filled with still air under normal conditions (Fig. 1). At the left boundary ($x = 0$), inflow conditions are specified with flow parameters corresponding to the flow behind a Mach 1.47 shock wave. At all other boundaries, impermeability conditions are set. The zero time is chosen for the time when the shock wave is ahead of the bed. In the computation time, the transmitted and reflected waves have no time to reach the domain boundaries $x = 0$ and $x = L$. The left boundary of the system of cylinders of diameter D has the coordinate $x_L = 0.4$ m. The length of the filled space is l and is a parameter being varied. The right boundary of the system of cylinders has the coordinate x_R and is at a distance of 0.4 m from the right boundary of the computational domain, which, thus, has a length of $L = 0.8 + l$.

For a constant intensity of the incident shock wave, the determining parameters of the problem are the permeability S of the system of cylinders (the ratio of the area occupied by gas in rectangle $[x_L; x_R] \times [0; H]$ to the area of this rectangle), its length l, and the cylinder diameter D [7]. The possible influence of the channel width H was also studied. For this purpose, a special procedure of arranging cylinders was developed, which requires only one of the parameters S, l, D, and H to be varied, leaving the other three unchanged. The centers of the cylinders are located at the nodes of a lattice of regular triangles. The coordinates of all the nodes of such a lattice are uniquely determined by the coordinates of any three pairwise neighboring nodes, e.g., $O_1(x_L + D/2, 0)$, $O_2(x_L + D/2 + \Delta\cos(\pi/6), \Delta\sin(\pi/6))$, and $O_3(x_L + D/2, \Delta)$ (Fig. 1). The cylinders whose distance from their centers to the upper or lower boundary of the extended computational domain are less than their radii are only partially contained within this domain. Tables 1–4 present the geometric parameters of all the performed experiments. For the considered geometric parameters, the values of the quantity $\theta = (1 - S)l/SD$ are also given, which were used for analyzing the obtained results. The described procedure of arranging cylinders is more flexible and functional than the approach proposed by Regele et al. [4]: the latter used a single arrangement of cylinders, which qualitatively imitated natural experiments for shock wave interaction with a particle cloud with a volume fraction of the dispersed phase of 0.15.

Table 1. Parameters of computational experiments with varying S ($H = 0.04$ m, $l = 0.06$ m, and $D = 0.006$ m)

Δ, 10^{-2} m	S	θ
3.5	0.971	0.30
1.7	0.894	1.19
1.2	0.756	3.23
0.9	0.566	7.67
0.7	0.319	21.32

The object of investigation was the transmitted and reflected waves formed following the interaction of an incident shock wave with a system of cylinders. The intensities of the two waves were determined by four pressure sensors installed at the points with the coordinates $(x_1, H/2)$, $(x_2, H/2)$, $(x_3, H/2)$, and $(x_4, H/2)$, where $x_1 = x_L - 0.33 = 0.07$ m, $x_2 = x_L - 0.13 = 0.27$ m, $x_3 = x_R + 0.13 = L - 0.27$ m, and $x_4 = x_R + 0.33 = L - 0.07$ m [7].

COMPUTATIONAL PROCEDURE

The mathematical model is based on a two-dimensional system of Euler equations, which are solved in the main computational domain obtained by subtracting the cylinders from the rectangle Π (see Fig. 1). The

computational algorithm is based on the Cartesian grid method and has been described in detail [6]. The main idea of the method is the use of square computational grids with special consideration for small grid cells obtained by the intersection of regular square cells and the curvilinear boundaries of the bodies; this consideration is made in terms of the so-called *h*-boxes [10]. The numerical fluxes are computed using Godunov's scheme [11] in Toro's implementation [12]. The computational algorithm allows the problems of shock wave propagation to be resolved in domains of arbitrary shape, while not requiring manual construction of the computational grid, which enables the performance of parametric studies in the formulation described in the previous section. Cell size for all calculations is 2×10^{-4} m.

The computational algorithm and its implementation in software were tested in our previous work [6] on a number of problems of shock wave theory. For the problems of regular and simple Mach reflection of a shock wave from a wedge, qualitatively correct shock-wave flow patterns were obtained. The discrepancies between the calculated and experimental [13] values of the gas density along the wedge in both cases did not exceed 8%. In the problem of shock wave interaction with a cylinder, the determined pressure distribution over the surface of the cylinder was within 1% of the results of detailed calculations using Navier–Stokes equations [14]. The problem of the interaction of a Mach 1.4 shock wave with an array of 16 cylinders located at nodes of a regular square lattice was also considered [15]. Chaudhuri et al. [15] solved this problem numerically, using two-dimensional Euler equations, with the immersed boundary method of high approximation order. The curves of the pressures at points upstream of, within, and downstream of the system of bodies were recorded. The calculated positions and amplitudes of pressure peaks differed from the published data [15] by no more than 5% and 10%, respectively.

The theoretical order of approximation of the algorithm is the first; nonetheless, it provides quantitative agreement with experimental data on the order of several percent. At the same time, use of the computational algorithm of the first order of approximation and Godunov's monotonic scheme for computing fluxes ensures the physical meaning of the obtained solutions and the absence of numerical oscillations, which is quite important in the considered problems of the interaction of many shock waves.

RESULTS OF COMPUTATIONAL EXPERIMENTS

The general evolution of the interaction of shock waves with the system of cylinders follows. Early in the interaction of the incident shock wave with the system of cylinders, a reflected wave forms, consisting of numerous components produced by reflections from individual cylinders. The intensity of the reflected wave increases over the course of the process due to the additional contribution made by perturbations resulting from the interaction of the leading wave with downstream cylinders. As a result, after some time, almost flat transmitted and collective reflected waves are formed. The wake flow behind the cloud is turbulized, and patterns resembling von Kármán vortex streets can be observed because the inviscid gas model is used in the presence of numerical viscosity in the computation.

Table 2. Parameters of computational experiments with varying D ($H = 0.04$ m, $l = 0.06$ m, and $S = 0.44$)

Δ, 10^{-2} m	D, 10^{-2} m	θ
3.5	2.75	2.78
1.7	1.36	5.61
1.2	0.91	8.39
0.9	0.68	11.23
0.7	0.58	14.14

Table 3. Parameters of computational experiments with varying l ($H = 0.04$ m, $D = 0.01$ m, and $S = 0.44$)

Δ, 10^{-2} m	l, 10^{-2} m	θ
1.3	2.2	2.80
"	4.4	5.60
"	6.6	8.4
"	8.8	11.2
"	11.0	14.0
"	13.2	16.8

Table 4. Parameters of computational experiments with varying H ($l = 0.06$ m, $D = 0.01$ m, and $S = 0.698$)

Δ, 10^{-2} m	H, 10^{-2} m
1.7	0.9
"	1.7
"	2.6
"	3.5
"	4.3

Figure 2 illustrates typical spatial pressure distributions in the performed computational experiments. At $S \approx 0.971$, a highly rarefied cloud of particles appears, and for $S \approx 0.319$, a dense one. The changes in the characteristics of the reflected and transmitted waves with varying S are easily seen. In the denser bed, the amplitude and velocity of the reflected wave are higher, and multidimensional effects are less pronounced. The behavior of the transmitted wave is the opposite. With decreasing bed permeability, the trans-

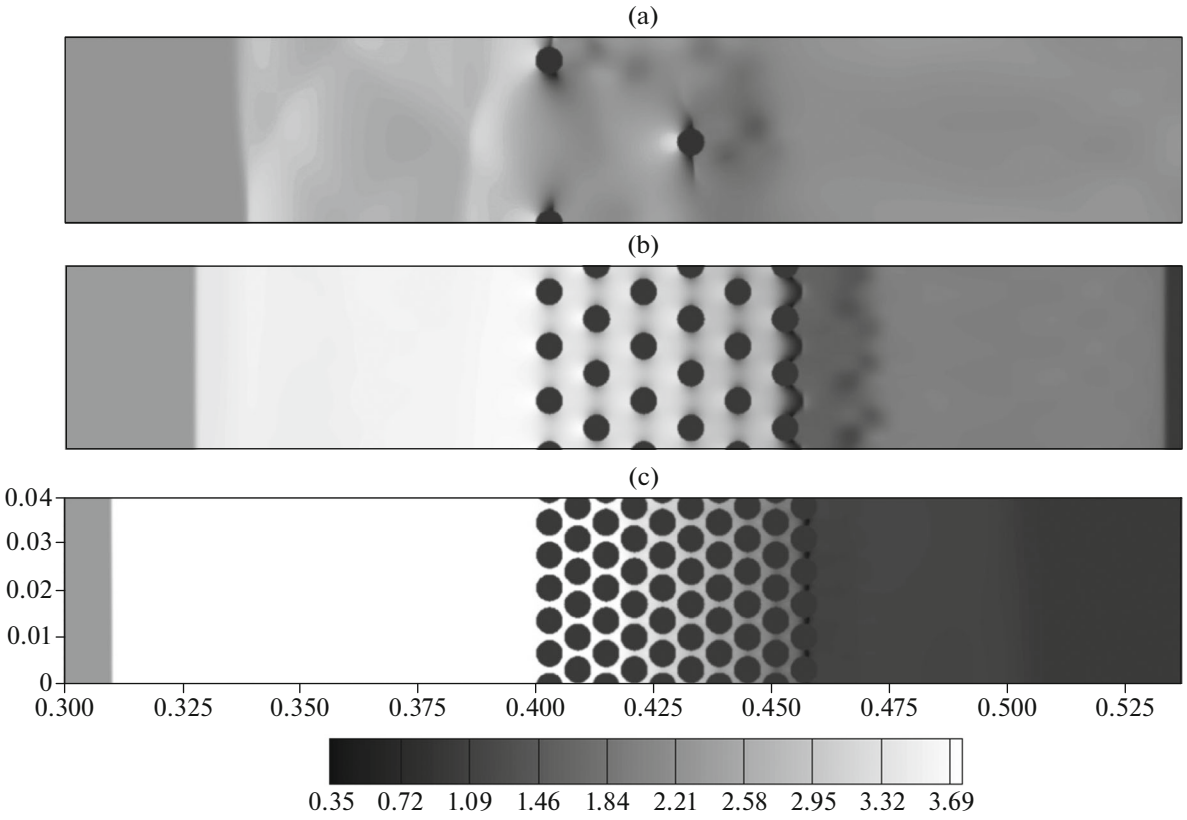

Fig. 2. Pressure distributions at the time 0.3 ms in the calculations with varying S (Table 1): (a) $S \approx 0.971$, (b) $S \approx 0.756$, and (c) $S \approx 0.319$. The numbers at the coordinate axes are distances in meters; the pressure scale is in atmospheres.

mitted wave weakens, its front becomes more diffuse, and turbulence effects in the wake behind the cloud are exhibited more strongly.

Figure 3 shows typical curves of the pressure at the pressure sensors for the calculation, the results of which are presented in Fig. 2b. Sensors 1 and 2 detect the reflected wave. Sensor 2, which is closer to the bed, indicates that, because of multiple reflections of the leading shock waves from the cylinders, the pressure reaches the medium level in a time on the order of 1 ms after the beginning of the shock wave interaction with the cylinders. The portion of the slow increase in the pressure to the medium level after the initial jump is due to multidimensional effects of the problem and cannot be obtained using one-dimensional models. Sensors 3 and 4 detect the transmitted wave, the parameters of the flow behind which reach the quasi-stationary level, experiencing oscillations related to the formation of vortex patterns in the wake downstream the bed.

From the curves of the pressure at the pressure sensors, the stationary pressures behind the reflected and transmitted waves were calculated by averaging over time and space. For example, the pressure behind the reflected wave is expressed as

$$P_{\text{refl}} = 0.5\left(\int_{t_{\text{refl}}}^{t_{\text{fin}}} P_1(t)\,dt + \int_{t_{\text{refl}}}^{t_{\text{fin}}} P_2(t)\,dt\right)\Big/(t_{\text{fin}} - t_{\text{refl}}),$$

where $P_i(t)$ is the pressure at the ith sensor as a function of time, t_{fin} is the time of the completion of the calculation, and t_{refl} is the time at which the reflected wave passed by sensors 1 and 2 (determined visually by analyzing the curves). For example, for Fig. 3, $t_{\text{fin}} =$ 2 ms and $t_{\text{refl}} = 1.5$ ms. The integrals were calculated numerically by the trapezoidal rule.

Figures 4 and 5 generalize the results of all the computational experiments in terms of overpressure behind the reflected and transmitted waves with respect to background normal pressure P_0: $\Delta_r = (P_{\text{refl}} - P_0)/P_0$, $\Delta_t = (P_{\text{trans}} - P_0)/P_0$. On the abscissas in these figures, the above-introduced dimensionless complex θ is plotted, which is proportional to that used for similar purposes by Medvedev et al. [7]. At $\theta < 7.5$, the points representing the results of the set of calculations with varying S have a significant distance from the other points. This is because this range corresponds to not too dense beds (Figs. 2a, 2b), whereas the parameter θ is a dimensionless criterion for dense beds.

In all the sets of calculations, the intensity of the reflected wave increases with increasing θ, i.e., with

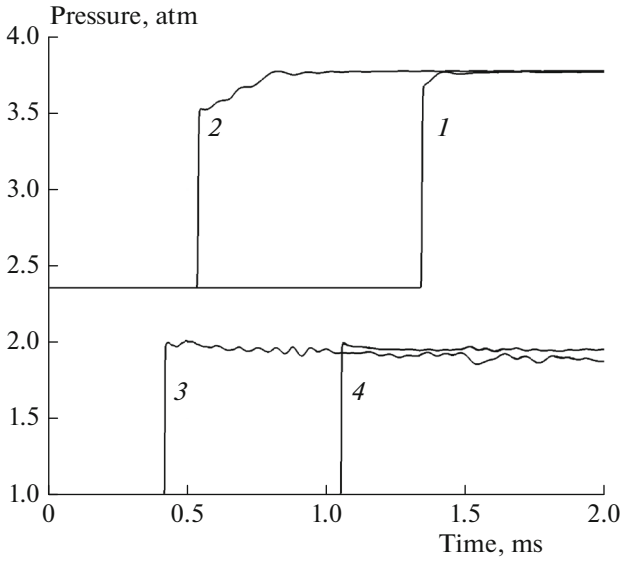

Fig. 3. Curves of the pressure at four pressure sensors (the number at a curve is the number of a sensor) for the case at $S \approx 0.756$ (Table 1).

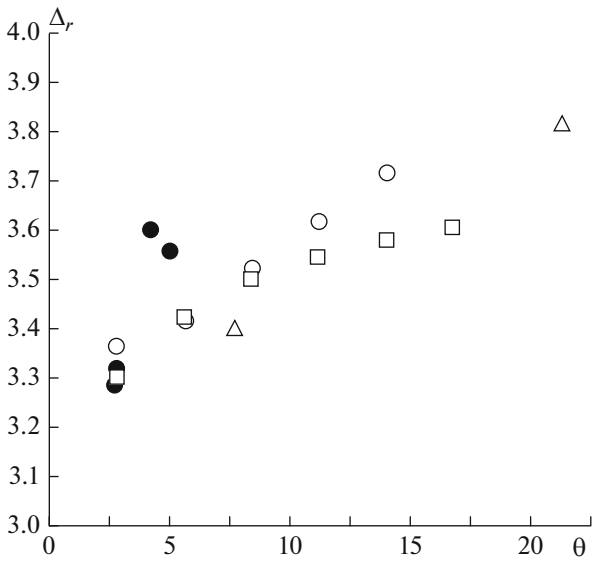

Fig. 4. Overpressures behind the reflected wave with varying S (triangles), D (circles), and l (boxes). Open symbols represent the results of the computational experiments; filled symbols represent experimental data [7].

increasing bed length and decreasing cylinder diameter and permeability. In Fig. 4, the level 4.0 corresponds to the overpressure behind the shock wave reflected from the impermeable wall. This figure also presents the experimental data [7] obtained for beds of granular media of minimum length. The discrepancy between the calculated and available experimental data within the range $2.5 < \theta < 5.0$ is within the range 5–7%.

Figure 5 illustrates the dependence of the overpressure on θ for the transmitted wave. Along with the calculated and experimental data, this figure also shows the analytically obtained curve [7]. This curve is the solution of the differential equation, which is obtained by substituting the Rankine–Hugoniot relations for the gas pressure, density, and velocity behind a shock wave in terms of the Mach number into the equation for the C_+-characteristic. For the drag coefficient of the bed, the published expression [16] is used. The discrepancy between the calculated and experimental data for the transmitted wave is much higher than that for the reflected one and can reach tens of percent at $\theta > 7.5$. Among the main causes of these discrepancies are the following:

—error related to the formulation of the problem, which describes a system of immobile round bodies arranged in a certain way. It is of interest to investigate systems of bodies arranged differently and bodies of a more complex shape.

—errors because the given studies were carried out in the two-dimensional formulation, using the inviscid gas model. An experimental study [17] showed that, for the same intensity of the incident shock wave (Mach 1.5), a system of spheres attenuates the shock wave more strongly than a system of cylinders of the same diameter and cross-sectional arrangement (Fig. 1 can present both a system of cylinders [top view] and a system of spheres). Although the permeability of the system of spheres is greater than that of the system of

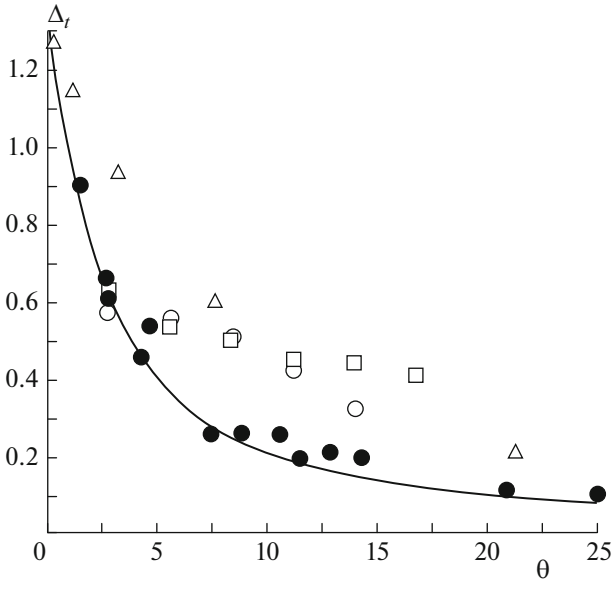

Fig. 5. Overpressures behind the transmitted wave with varying S (triangles), D (circles), and l (boxes). Open symbols represent the results of the computational experiments; filled symbols represent the experimental data [7]; the line represents the theoretical curve [7].

cylinders (0.46 as against 0.37 in the performed experiments), the surface area per unit volume for spheres is larger, which ultimately results in a greater attenuation of the incident shock wave. To reproduce this effect, it may be necessary to use a viscous gas model. The results presented in Fig. 5 qualitatively agree with the conclusions of the experimental study [17].

The agreement between the calculated, experimental, and theoretical results is the best within the same range as for the reflected wave: $2.5 < \theta < 5.0$. This can probably be explained by the fact that this θ range corresponds to beds of minimum length and bodies of maximum size; under such conditions, the formulation of the problem is close to the case of perforated plates, for which the two-dimensional mathematical model used seems to be more natural.

Computational experiments with varying channel widths demonstrated that the intensity of the reflected wave is independent of this parameter to within fractions of a percent of average overpressure. The intensity of the transmitted wave tends to decrease with increasing channel width to within several percent of average overpressure, which may be attributed to the presence of turbulent phenomena behind the bed.

CONCLUSIONS

A parametric numerical study was conducted of the interaction of a shock wave with a system of cylinders, modeling a bed of a granular medium with a varying bed length and permeability, cylinder diameter, and channel length. Each computational experiment was the calculation of the characteristics of the shock wave propagating in the domain obtained by subtracting the system of cylinders from a rectangle using a numerical integration of the Euler equations with the Cartesian grid method. This computational procedure is efficient for the study of both rarefied and dense beds. The results of the computational experiments in terms of overpressure behind the reflected and transmitted waves were generalized using the dimensionless criterion $\theta = (1 - S)l/SD$, where S is the permeability of the system of cylinders, l is the length of the system, and D is the diameter of a cylinder.

All sets of calculations for the reflected wave showed an increase in its intensity with increasing θ, i.e., with increasing bed length and decreasing cylinder diameter and permeability. The relative discrepancy between the calculated and available experimental data within the range $2.5 < \theta < 5.0$ is within the range 5–7%.

The discrepancy between the calculated and experimental data for a transmitted wave is much greater than that for a reflected one, and it can reach tens of percent at $\theta > 7.5$. The agreement between the calculated, experimental, and theoretical results is best within the same range as for the reflected wave: $2.5 < \theta < 5.0$.

ACKNOWLEDGMENTS

This work was supported in part by the Council for Grants of the President of the Russian Federation for State Support of Young Russian Scientists and State Support of Leading Scientific Schools of the Russian Federation (grant no. 14.W01.16.6756-MK) and in part by a state assignment for the Institute for Computer Aided Design, Russian Academy of Sciences, Moscow, Russia.

REFERENCES

1. *Handbook of Shock Waves,* Ed. by G. Ben-Dor, O. Igra, and T. V. Elperin (Academic, New York, 2001), Vol. 2.
2. I. A. Bedarev, A. V. Fedorov, and V. M. Fomin, Combust. Explos., Shock Waves **48**, 446 (2012).
3. I. A. Bedarev and A. V. Fedorov, J. Appl. Mech. Tech. Phys. **56**, 750 (2015).
4. J. D. Regele, J. Rabinovitch, T. Colonius, et al., Int. J. Multiphase Flow **61**, 1 (2014).
5. Y. Mehta, C. Neal, T. L. Jackson, et al., Phys. Rev. Fluids **1**, 054202 (2016).
6. D. A. Sidorenko and P. S. Utkin, Vychisl. Metody Program. **17**, 353 (2016).
7. S. P. Medvedev, S. M. Frolov, and B. E. Gel'fand, Inzh.-Fiz. Zh. **58**, 924 (1990).
8. O. A. Mirova, A. L. Kotel'nikov, V. V. Golub, and T. V. Bazhenova, High Temp. **54**, 905 (2016).
9. P. N. Krivosheyev, A. O. Novitski, O. G. Penyazkov, et al., in *Proceedings of the 26th International Colloquium on the Dynamics of Explosions and Reactive Systems ICDERS, Boston, USA, July 30–Aug. 4, 2017,* Paper No. 1022.
10. M. Berger and C. Helzel, SIAM J. Sci. Comput. **34**, 861 (2012).
11. S. K. Godunov, A. V. Zabrodin, M. Ya. Ivanov, et al., *Numerical Solution of Multidimensional Problems of Gas Dynamics* (Nauka, Moscow, 1976) [in Russian].
12. E. F. Toro, *Riemann Solvers and Numerical Methods for Fluid Dynamics,* 3rd ed. (Springer, Berlin, Heidelberg, 2009).
13. H. M. Glaz, P. Colella, I. I. Glass, et al., Proc. R. Soc. London, A **398**, 117 (1985).
14. D. Drikakis, D. Ofengeim, E. Timofeev, et al., J. Fluids Struct. **11**, 665 (1997).
15. A. Chaudhuri, A. Hadjadj, O. Sadot, et al., Int. J. Numer. Meth. Eng. **89**, 975 (2012).
16. S. Ergun, Chem. Eng. Progress **48**, 89 (1952).
17. A. Abe, K. Takayama, and K. Itoh, WIT Trans. Model. Simul. **30**, 209 (2001).

Translated by V. Glyanchenko